1. Title Page.

Altered Expression and Function of Hepatic Transporters in a Rodent Model of Polycystic Kidney Disease

Jacqueline Bezençon, James J. Beaudoin, Katsuaki Ito, Dong Fu, Sharin E. Roth, William J. Brock, Kim L. R. Brouwer

Division of Pharmacotherapy and Experimental Therapeutics, UNC Eshelman School of Pharmacy, University of North Carolina, Chapel Hill, North Carolina, USA (J.B., J.J.B., K.I., D.F., K.L.R.B.); DMPK Research Department, Teijin Pharma Limited, Hino, Tokyo, Japan (K.I.); Otsuka Pharmaceutical Development & Commercialization, Inc., Rockville, Maryland, USA (S.E.R.); Brock Scientific Consulting, Montgomery Village, Maryland, USA (W.J.B)

DMD Fast Forward. Published on June 3, 2019 as DOI: 10.1124/dmd.119.086785
This article has not been copyedited and formatted. The final version may differ from this version.

2. Running Title Page

a) Running title (58 out of 60 characters including spaces): Running Title: Polycystic Kidney Disease Alters Hepatic Drug Transporters

b) Corresponding author: Kim L. R. Brouwer, UNC Eshelman School of Pharmacy, The University of North Carolina at Chapel Hill, CB #7569 Kerr Hall, Chapel Hill, NC 27599-7569. Phone: (919) 962-7030. Fax: (919) 962-0644. E-mail: kbrouwer@email.unc.edu

c) Number of text pages: (including references, footnotes, figure legends and tables; excluding figures and supplemental data)

Number of tables: 2

Number of figures: 6

Number of references: 51

Number of words in the Abstract: 249 out of 250 used.

Number of words in the Introduction: 748 out of 750 used.

Number of words in the Discussion: 850 out of 1500 used.

d) Abbreviations: ADPKD: autosomal dominant polycystic kidney disease; ALT: alanine aminotransferase; ARPKD: autosomal recessive polycystic kidney disease; Bsep: bile salt export pump; CDCA: chenodeoxycholic acid; CDF: 5(6)-carboxy-2',7'-dichlorofluorescein; CL_{UP}: uptake clearance; DCA: deoxycholic acid; Gapdh: glyceraldehyde 3-phosphate dehydrogenase; GCDCA: glycochenodeoxycholic acid; GSH: reduced glutathione; GSSG: glutathione disulfide; HPR: horseradish peroxidase; IPL: isolated perfused liver; K_{BL}:

basolateral efflux rate constant; K_{Bile}: biliary efflux rate constant; $K_{Lag,Bile}$: transit rate constant for biliary excretion; LC-MS/MS: liquid chromatography–tandem mass spectroscopy; LDH: lactate dehydrogenase; LLOQ: lower limit of quantitation; Mrp: multidrug resistance-associated protein; Mdr: multidrug resistance; m/z, mass-to-charge ratio; NADPH: nicotinamide adenine dinucleotide phosphate, reduced form; Ntcp: Na^+-taurocholate co-transporting polypeptide; Oatp: organic anion transporting polypeptide; Ost: organic solute transporter; P-gp: P-glycoprotein; PCK: polycystic kidney; PKD: polycystic kidney disease; *PKD1/2*: Polycystic Kidney Disease 1/2; *PKHD1*: Polycystic Kidney and Hepatic Disease 1; PLD: polycystic liver disease; SRM: selected reaction monitoring; TBS-T: Tris-buffered saline Tween 20; TCDCA: taurochenodeoxycholic acid; UPLC: ultra-performance liquid chromatography; WT: wild-type (Sprague-Dawley rats).

3. Abstract

Autosomal dominant polycystic kidney disease (ADPKD) is a common form of inherited polycystic kidney disease (PKD) and is a leading cause of kidney failure. Patients with ADPKD develop fluid-filled cysts in their kidneys, and often form cysts in their liver and other organs. Previous data have shown that bile acids are increased in the liver of polycystic kidney (PCK) rats, a rodent model of ADPKD; these changes may be associated with alterations in liver transporter expression and function. However, the impact of PKD on hepatic transporters has not been characterized. Therefore, this preclinical study was designed to investigate hepatic transporter expression and function in PCK compared to wild-type (WT) Sprague Dawley rats. Transporter gene expression was measured by qPCR, and protein expression was quantified by western blot and LC-MS/MS-based proteomic analysis in rat livers. Transporter function was assessed in isolated perfused livers (IPLs), and biliary and hepatic total glutathione content were measured. Protein expression of Mrp2 and Oatp1a4 was decreased 3-fold and 2.9-fold, respectively, in PCK rat livers based on western blot analysis. Proteomic analysis confirmed a decrease in Mrp2 and a decrease in Oatp1a1 expression (PCK/WT ratios of 0.368±0.098 and 0.563±0.038, respectively; mean±SD). The biliary excretion of 5(6)-carboxy-2',7'-dichlorofluorescein (CDF), a substrate of Oatp1a1, Mrp2, and Mrp3, was decreased 28-fold in PCK compared to WT rat IPLs. Total glutathione was significantly reduced in the bile of PCK rats. Differences in hepatic transporter expression and function may contribute to altered disposition of Mrp2 and Oatp substrates in PKD.

4. Visual Abstract (please see supplemental file)

5. Introduction

Polycystic kidney disease (PKD) is the fourth leading cause of kidney failure worldwide (Chebib and Torres, 2016). Autosomal dominant polycystic kidney disease (ADPKD) is caused by mutations in the polycystin-1 or -2 (*PKD1* or *PKD2*) genes and is the most common form of PKD (prevalence of >1 in 1,000 people). Autosomal recessive polycystic kidney disease (ARPKD) is a rare neonatal form of PKD (Halvorson et al., 2010) and is caused by mutations in the polycystic kidney and hepatic disease 1 (*PKHD1*) gene (Harris and Torres, 2009; Hartung and Guay-Woodford, 2014). Despite the genetic differences between ADPKD and ARPKD, both diseases are associated with fluid-filled cysts and renal impairment. By the age of 70, 50% of patients with ADPKD require dialysis or kidney transplantation (Halvorson et al., 2010). Hepatic cysts are the most common extra-renal manifestation in patients with ADPKD and occur in 75-90% of patients with ADPKD. Hepatic cysts typically develop later than renal cysts (Chauveau et al., 2000; Harris and Torres, 2009; Cnossen and Drenth, 2014) and their presence is generally considered benign, although hepatic biochemical abnormalities have been reported (Everson et al., 1988; Qian et al., 2003; Hogan et al., 2015). Increased serum γ-glutamyl transferase or alkaline phosphatase of ~2-5 times the upper limit of normal has occurred in some patients with large polycystic livers (Chauveau et al., 2000; Qian et al., 2003). Although the impact of PKD on the hepatobiliary disposition of drugs has not been evaluated in humans, a case report in a patient with ADPKD who exhibited increased hepatic retention of the MRP2 probe substrate ^{99m}Tc-mebrofenin suggests that multidrug resistance-associated protein (MRP) 2 function may be impaired (Salam and Keeffe, 1989).

Until recently, ADPKD therapy has been directed only towards symptomatic treatment. Tolvaptan, an oral, selective vasopressin V2-receptor antagonist, has been shown to slow disease progression in patients with ADPKD, and was approved in April 2018 by the FDA to slow kidney function decline in adults at risk for rapidly progressing ADPKD (US FDA, 2018). However, in two pivotal clinical trials (Torres et al., 2012; Torres et al., 2017), the incidence of alanine aminotransferase (ALT) elevations was ~5% higher in patients receiving tolvaptan compared to placebo. Alternate causes for ALT elevations were ruled out and, therefore, tolvaptan has been associated with liver injury in patients with ADPKD (Watkins et al., 2015). One possible explanation could be that tolvaptan interacts with hepatic transport proteins, especially bile acid transporters. *In vitro* studies indicated that tolvaptan is a substrate and competitive inhibitor of P-glycoprotein (P-gp, MDR1/ABCB1) (Shoaf et al., 2011), while tolvaptan and the primary plasma metabolites, DM-4103 and DM-4107, inhibit several hepatic transporters. For example, DM-4103 strongly inhibited the hepatic bile acid uptake transporter Na^+-taurocholate co-transporting polypeptide (NTCP/*SLC10A1*), the canalicular bile salt export pump (BSEP/ABCB11), and the basolateral efflux transporter MRP4 (Slizgi et al., 2016). Interestingly, elevated liver enzymes have not been reported in non-ADPKD patients treated with tolvaptan (Watkins et al., 2015). Concomitantly, PKD may alter the function of hepatic transport proteins.

Polycystic kidney (PCK) rats have the same genetic defect as in ARPKD (*i.e.*, *PKHD1*) and exhibit similar hepatorenal abnormalities (*e.g.,* congenital hepatic fibrosis and development of cysts) as patients with ARPKD or ADPKD (Lager et al., 2001, Katsuyama et al., 2000; Masyuk et al., 2004). Various bile acids that are substrates for hepatic transporters (Dawson et al., 2009) are increased in PCK rat serum and liver (Ruh et al., 2013; Munoz-Garrido et al., 2015; Brock et

al., 2018). In addition, serum bilirubin concentrations are increased in PCK rats, suggesting impaired Mrp2 function (Mason et al., 2010; Shimomura et al., 2015). Furthermore, the biliary clearance of tolvaptan was significantly decreased in isolated perfused livers (IPLs) from PCK compared to wild-type (WT) rats (Beaudoin et al., 2018). The IPL is a physiologically relevant *ex situ* model (Brouwer and Thurman, 1996) that has been used to evaluate the hepatic transport and metabolic properties of various compounds (Chandra et al., 2005a; Miranda et al., 2008; Pfeifer et al., 2013).

This preclinical study was designed to elucidate possible mechanisms of altered hepatobiliary disposition of drugs and endogenous compounds in a rodent model of ADPKD. Hepatic transporter mRNA and protein expression were investigated in PCK and WT rat livers. Functional changes in organic anion transporting polypeptides (Oatps), Mrp2 and Mrp3 (Zamek-Gliszczynski et al., 2003) were measured in WT and PCK rat IPLs using 5(6)-carboxy-2',7'-dichlorofluorescein (CDF), a fluorescent and metabolically stable probe substrate. In addition, hepatic and biliary total glutathione was quantified in WT and PCK rats.

DMD Fast Forward. Published on June 3, 2019 as DOI: 10.1124/dmd.119.086785
This article has not been copyedited and formatted. The final version may differ from this version.

6. Materials and Methods

Chemicals and Reagents. CDF was obtained from Sigma-Aldrich (St. Louis, MO). All other chemicals and reagents were of analytical grade or higher and were readily available from commercial sources. The stable isotope labeled peptides for *Na^+/K^+ ATPase/*Na^+/K^+ ATPase, *Slc1ab1/*Oatp1a1, *Slc1a4/*Oatp1a4, *Slc1b2/*Oatp1b2, *Slc210a1/*Ntcp, *Abcc2/*Mrp2, *Abcc3/*Mrp3, *Abcb11/*Bsep (Table 1) were generated by a peptide synthesis platform (PEPscreen®, Custom Peptide Libraries, Sigma-Genosys, Sigma-Aldrich, St. Louis, MO).

Animals. Male WT Sprague-Dawley or PCK (PCK/CrljCrl-*Pkhd1*^{pck}/Crl) rats were purchased from Charles River Laboratories (Wilmington, MA). Rats were housed in a constant alternating 12-hr light/dark cycle and allowed water and food *ad libitum* and acclimated for a minimum of 1 week prior to experimentation. All animal procedures complied with the guidelines of the Institutional Animal Care and Use Committee (IACUC, University of North Carolina, Chapel Hill, NC). Single-pass IPL procedures were performed, and bile and liver tissue samples were collected at 16 weeks of age because the expected pathological changes (*e.g.*, hepatic cysts) in PCK rats are well defined at this age (Lager et al., 2001; Mason et al., 2010).

qRT-PCR Analysis. Total RNA from WT and PCK rat liver tissue samples were isolated using the RNeasy Plus Mini Kit (Qiagen GmbH, Hilden, Germany) according to the manufacturer's instructions. The concentration and purity of isolated RNA were analyzed with a NanoDrop spectrophotometer (ND-1000; Thermo Fisher Scientific, Waltham, MA). RNA was converted to cDNA and cDNA was analyzed as described previously (Jackson et al., 2016). Briefly, reverse transcription was performed using High Capacity cDNA Archive Kit, following the manufacturer's instructions (Life Technologies, Carlsbad, CA). *Abcc2* (Mrp2), *Abcc3* (Mrp3), *Abcb1b* (Mdr1), *Slco1a1* (Oatp1a1), *Slco1a2* (Oatp1a4), *Slco1b2* (Oatp1b2), *Slc51a* (Ostα) and *Slc51b* (Ostβ)

DMD Fast Forward. Published on June 3, 2019 as DOI: 10.1124/dmd.119.086785
This article has not been copyedited and formatted. The final version may differ from this version.

cDNA were analyzed from each sample in duplicate or triplicate using gene-specific Taqman® assays (Mrp2, Rn00563231_m1; Mrp3, Rn01452854; Mdr1, Rn01529252; Oatp1a1, Rn00755148; Oatp1a4, Rn00756233; Oatb1b2, Rn01492635; Ostα, Rn01763289_m1; Ostβ, Rn01767005_m1, Thermo Fisher Scientific, Waltham, MA) and a Real-Time PCR System (QuantStudio 6 Flex, Life Technologies, Carlsbad, CA). The expression level of the studied genes was normalized against the selected reference gene, glyceraldehyde 3-phosphate dehydrogenase (Gapdh, Rn01775763_g1, Thermo Fisher Scientific, Waltham, MA), and the relative quantification ($2^{-\Delta\Delta Ct}$, fold difference in WT relative to PCK) was calculated against the calibrator sample (cDNA from WT rat liver sample). No-template control from reverse transcription was present on each PCR plate.

Western Blot Analysis. Membrane proteins from rat liver samples (from the median liver lobe) were extracted using a proteoExtract® native membrane protein extraction kit (Catalog No. 444810; Calbiochem, San Diego, CA). The total protein was determined by Pierce BCA Protein assay kit (Thermo Fisher Scientific, Waltham, MA) using the manufacturer's protocol. Samples for western blots were prepared according to the manufacturer's instructions (Life Technologies, Carlsbad, CA); 35 µg was loaded onto Bis-Tris 4-12% (Oatp1a1, Oatp1a4, Oatp2b1, Ostβ, Mdr1) or Tris Acetate 7% (Mrp2, Mrp3) gels. After electrophoresis, transfer of proteins to polyvinylidene fluoride membranes according to standard procedures was performed. Each protein was analyzed separately on a different membrane, and Na^+/K^+ ATPase was probed on the same blot as the respective protein and used as the loading control. The membranes were incubated with anti-Oatp1a1 (1:200, AB3670P, Millipore, Burlington, MA), anti-Oatp1a4 (1:500, AB3672P, Millipore, Burlington, MA), anti-Oatp1b2 (1:100, sc-376904, Santa Cruz Biotechnology, Dallas, TX), anti-Mrp3 (1:1,000, 399095, Cell Signaling Technology, Danvers, MA), anti-Ostβ antibody

DMD Fast Forward. Published on June 3, 2019 as DOI: 10.1124/dmd.119.086785
This article has not been copyedited and formatted. The final version may differ from this version.

(1:150, Sigma-Aldrich, St. Louis, MO), anti-Mrp2 (1:20, MC-206, Kamiya Biochemical Company, Seattle, WA), anti-Mdr1b (1:100, sc-55510, Santa Cruz Biotechnology, Dallas, TX), or anti-N^+/K^+ ATPase (1:5,000, sc-28800, Santa Cruz Biotechnology, Dallas, TX) overnight in diluted 5% (w/v) bovine serum albumin (BSA)-tris-buffered saline Tween 20 (TBS-T). After washing, the blots were probed with horseradish peroxidase (HRP)-conjugated anti-rabbit (for Oatp1a1, Oatp1a4, Ostβ, and Mrp3, 1:7,000, sc-2030, Santa Cruz Biotechnology, Dallas, TX) or HRP-conjugated anti-mouse IgG secondary antibody (for Oatp1b2, Mdr1, and Na^+/K^+ ATPase 1:10,000, 115-035-003, Jackson ImmunoResearch Laboratories, West Grove, PA) in 5% milk for 1 h at room temperature. Detection was enhanced using chemiluminescence reagents (ECLTM Select, GE Healthcare Bio-Sciences, Piscataway, NJ) and measured with ImageLab software version 4.1 (Bio-Rad, Hercules, CA). The data were normalized to loading control (Na^+/K^+ ATPase) using densitometric analysis to compare protein expression between WT and PCK rats with ImageJ version 1.51 (National Institutes of Health, USA).

Protease Digestion and Solid Phase Extraction. As described previously (Malinen et al., 2018), membrane protein samples, as prepared for western blot, were diluted to a concentration of 100 µg membrane protein/100 µl and mixed in ammonium bicarbonate buffer (25 mM) containing 5% deoxycholate and 10 mM dithiothreitol. After incubation for 40 min at 56°C, iodoacetamide was added (final concentration of 15 mM) and the sample was incubated for 30 min at room temperature. For protease digestion, samples were diluted 5-fold with ammonium bicarbonate buffer and digested using Lys-C protease (Thermo Fisher Scientific, Waltham, MA) in a protein:protease ratio of 20:1. After incubation for 4 hrs at 37°C, a protein:trypsin ratio of 20:1 was applied followed by incubation overnight at 37°C. Formic acid was added (final concentration 2% v/v) to stop the protease reaction. The mixture of stable isotope-labeled

peptides (Table 1) was used as internal standards. For solid phase extraction, the cartridge (Oasis HLB, Waters Co., Milford, MA) was pre-washed with methanol and equilibrated with 0.1% formic acid in water (v/v) before the sample was added. After washing the cartridge with 0.1% formic acid in water (v/v), the peptides were eluted by adding 0.1% formic acid in acetonitrile (v/v). A centrifugal evaporator (Speedvac high-capacity concentrator, Thermo Fisher Scientific, Waltham, MA) was used to evaporate the eluate, and samples were reconstituted in 0.1% formic acid and 2% acetonitrile in water (v/v/v). After centrifugation (21,000 g, 1 min), the supernatant was analyzed by LC-MS/MS.

Signature Peptide Selection and Quantification by LC-MS/MS. Signature peptides and internal standard peptides for each transporter (Li et al., 2008; Li et al., 2009; Uchida et al., 2011; Prasad et al., 2014; Wang et al., 2015) (Table 1) were analyzed by LC-MS/MS [Thermo Scientific™ TSQ Quantum Ultra Triple Quadrupole mass spectrometer (Thermo Fisher Scientific, Waltham, MA) with nanoAcquity UPLC (Waters Co., Milford, MA)] in the selected reaction monitoring (SRM) mode with three sets of transitions. As described previously (Malinen et al., 2018), samples were injected onto the Waters® ACQUITY UPLC M-Class Symmetry C18 Trap Column (5 µm, 180 µm x 20 mm, Waters Co., Milford, MA) in 98% mobile phase A (0.1% formic acid in water) and 2% B (0.1% formic acid in acetonitrile) (flow rate of 5 µL/min for 3 min). The peptides were first trapped and then separated on an analytical column (Waters® ACQUITY UPLC HSS T3 nanoACQUITY Column, 1.8 µm, 100 µm x 100 mm, Waters Co.) at a flow rate of 0.6 µL/min, and a linear gradient of mobile phase B concentration of 5% for 0-1 min; 5-35% for 1-25 min, 35-90% for 25-25.5 min, followed by the washing step using 90% mobile phase B for 4.5 min, and re-equilibrium for 10 min. Xcalibur software (Thermo Fisher Scientific, Waltham, MA) was used to process the data by integrating the peak areas generated from the

reconstructed ion chromatograms for the analyte peptides and their respective internal standards. Transporters were considered to be expressed when analyte peaks were detected in three sets of transitions. Then, the peak area ratios of the analyte peptide to its internal standard were calculated for three sets of transitions. To compare the expression levels of transporters among samples, the PCK/WT ratio was calculated with the peak area mean from each transition (n=3) and compared to Na^+/K^+ ATPase PCK/WT ratio, assuming there was no change in the Na^+/K^+ ATPase protein in PCK compared to WT rat livers. The corresponding peptides, heavy-labeled at [$^{13}C_6{}^{15}N_2$]-lysine (**K$^+$**) and [$^{13}C_6{}^{15}N_4$]-arginine (**R$^+$**) residues, were used as the internal standards.

Total Glutathione Determination. Total glutathione concentrations (reduced glutathione, GSH plus glutathione disulfide, GSSG) were determined according to the manufacturer's instructions (CS0260, Sigma-Aldrich, St. Louis, MO). Briefly, 10 µl of blank bile (collected before IPLs) and 40 to 200 mg of liver tissue were diluted with 5% sulfosalicylic acid solution. The solutions were vigorously vortexed and left for 10 min on ice prior to centrifugation (10,000 x g) for 10 min at 4°C. The supernatant volume was measured and samples were loaded on a 96 well plate and incubated for 5 min with the working solution containing 95 mM potassium phosphate, 0.95 mM EDTA, 0.031 mg/mL 5,5'-dithiobis(2-nitrobenzoic acid), 0.115 units/mL glutathione reductase from baker's yeast, and 0.24% 5-sulfosalicylic acid. After adding NADPH to a final concentration of 0.038 mg/mL and mixing, the samples were read at 412 nm at 1-min intervals for 5 min with a spectrophotometer (PowerWave XS, Biotek, Winooski, VT). Concentrations were calculated according to the manufacturer's instructions.

CDF Disposition in Rat IPLs. WT and PCK rat livers were perfused as described previously (Brouwer and Thurman, 1996; Chandra et al., 2005a). Briefly, animals were anesthetized with

ketamine:xylazine (60:12 mg/kg i.p.) and the bile duct and portal vein were cannulated. Following cannulation and the collection of blank bile, the livers were perfused *ex situ* in a single-pass manner with continuously oxygenated Krebs-Henseleit buffer (38 mL/min). First, livers were perfused with blank perfusate for a 15-min equilibration period, then with CDF (~1 μM) for 30 min followed by perfusion for 20-min with CDF-free buffer. Outflow perfusate and bile were collected continuously. Outflow perfusate was collected for 50 min by sampling directly from the perfusate flowing out of the vena cava; bile was collected over 5-min intervals for 50 min. Liver viability was monitored by gross morphology, portal perfusion pressure (<15 cm H_2O), bile flow (>2 μL/min (Zhang et al., 2016)), and by lactate dehydrogenase (LDH) levels in the outflow perfusate measured by the Pierce™ LDH Cytotoxicity Assay Kit (Thermo Fisher Scientific, Waltham, MA) per the manufacturer's instructions.

CDF Sample Preparation. Perfusate and bile samples were thawed and diluted with buffer and analyzed for CDF by fluorescence spectroscopy using a Cytation 3 imaging reader (BioTek, Winooski, VT) at wavelengths of 485 nm (excitation) and 518 nm (emission). Two standard curves were prepared by diluting CDF in perfusate buffer, and blank bile diluted in perfusate buffer (1:100). The lower limit of quantitation (LLOQ) was 0.1 nM for the perfusate buffer matrix and 10 nM for the diluted blank bile matrix.

Pharmacokinetic Analysis. The hepatobiliary disposition of CDF was analyzed using a pharmacokinetic modeling approach. The compartmental model, consisting of a sinusoidal, hepatocellular and a bile compartment (scheme depicted in Figure 1), was fit simultaneously to the average CDF outflow perfusate and biliary excretion rate data from rat IPLs. Data from WT and PCK rat IPLs were fit separately. A combined additive and multiplicative residual error model [Phoenix® WinNonlin® version 8.1 (St. Louis, MO)] was used to estimate parameters listed in

Table 2. The bile compartment for PCK rat IPLs consisted of five transit compartments in order to describe the delay in the detection of CDF in bile. The differential equations, assuming linear conditions and an initial concentration of zero in all compartments, are as follows:

WT and PCK sinusoidal compartment:

$$\frac{dX_S}{dt} = Q \cdot C_{in} + K_{BL} \cdot X_H - (CL_{UP} + Q) \cdot C_S \quad (1)$$

WT and PCK hepatocellular compartment:

$$\frac{dX_H}{dt} = CL_{UP} \cdot C_S - (K_{BL} + K_{Bile}) \cdot X_H \quad (2)$$

WT and PCK concentration data in outflow perfusate expressed as $\frac{dX}{dt}$:

$$\frac{dX_{out}}{dt} = Q \cdot C_S \quad (3)$$

WT concentration data in bile expressed as $\frac{dX}{dt}$:

$$\frac{dX_{Bile}}{dt} = K_{Bile} \cdot X_H \quad (4)$$

PCK transit compartment 1 following biliary excretion:

$$\frac{dX_{Bile,1}}{dt} = K_{Bile} \cdot X_H - K_{Lag,Bile} \cdot X_{Bile,1} \quad (5)$$

PCK transit compartments 2-5 following biliary excretion:

$$\frac{dX_{Bile,n}}{dt} = K_{Lag,Bile} \cdot X_{Bile,n-1} - K_{Lag,Bile} \cdot X_{Bile,n} \quad (6)$$

PCK concentration data in bile expressed as $\frac{dX}{dt}$:

$$\frac{dX_{Lag,Bile}}{dt} = K_{Lag,Bile} \cdot X_{Bile,5} \quad (7)$$

where $\frac{dX}{dt}$ represents the rate of change of CDF in a specific compartment with respect to time and X_S, X_H, X_{out}, X_{Bile}, $X_{Bile,n}$, and $X_{Lag,Bile}$ represent the CDF mass in the sinusoidal space, hepatocellular space, outflow perfusate, bile, nth biliary transit compartment, and the bile

DMD Fast Forward. Published on June 3, 2019 as DOI: 10.1124/dmd.119.086785
This article has not been copyedited and formatted. The final version may differ from this version.

compartment after the lag in biliary detection has been described, respectively. Other parameters are defined as follows:

C_{in}: inflow concentration

CL_{UP}: uptake clearance from the sinusoidal space to the hepatocellular space

K_{BL}: basolateral efflux rate constant from the hepatocellular space to the sinusoidal space

K_{Bile}: biliary efflux rate constant from the hepatocellular space to bile

$K_{Lag,Bile}$: transit rate constant for the biliary excretion of CDF

C_S, calculated as X_S/V_S, represents the extracellular concentration in the sinusoidal compartment and was assumed to be equal to C_{out}. The sinusoidal space was assumed to be in equilibrium with the extracellular volume of the liver, V_S, and was estimated as 20% of the total liver mass (Watanabe et al., 2009; Hobbs et al., 2012), which was converted to total liver volume (V_L) using the average density of rat liver (1.084 g/mL) (Pretlow II and Pretlow, 1987). The observed outflow perfusate rate data was described by the perfusate flow rate multiplied by the concentration in the sinusoidal compartment ($Q \cdot C_S$), while the observed biliary excretion rate data were described by dX_{Bile}/dt and $dX_{Lag,Bile}/dt$ for WT and PCK rat IPLs, respectively.

Data Analysis. All data are presented as mean and standard deviation (SD) from *n*=3 livers per group (WT and PCK). Statistical tests [unpaired, two-tailed *t*-tests (α=0.05) corrected (only for proteomics data) by using the Bonferroni-Dunn multiple comparison method] were performed using GraphPad Prism 7.0b for Windows, GraphPad Software, La Jolla, CA. Final parameter estimates were significantly different if the 95% confidence intervals (CIs) between the WT and PCK groups did not overlap (Schenker, 2001).

7. Results

Transporter Gene Expression in WT Compared to PCK Rat Livers. The relative transporter gene expression in WT compared to PCK rat livers, assessed by qPCR, is shown in Figure 2. The mRNA levels of both *Slc21a1* (Oatp1a1*)* and *Slco1a4* (Oatp1a4) were significantly decreased in PCK rat livers by 2.6- and 2.5-fold, respectively. *Slc51a (*Ostα), *Slc51b (*Ostβ), and Abcc3 (Mrp3) mRNA levels were significantly increased by 88-, 28-, and 9-fold, respectively, in livers from PCK compared to WT rats. *Abcc2 (*Mrp2) and *Slco1b2 (*Oatp1b2) mRNA levels were decreased by 2.4- and 1.5-fold, and *Abcb1b* (Mdr1b) showed a 71-fold increase in PCK compared to WT rat livers, but differences were not statistically significant.

Transporter Protein Expression in WT Compared to PCK Rat Livers. Protein expression levels were determined using western blot analysis (Figure 3) and LC-MS/MS proteomic analysis (Figure 4). Immunoblot analysis of liver tissue from WT and PCK rats revealed a significant decrease in Oatp1a4 and Mrp2 (2.9- and 3.0-fold, respectively; Figure 3) in PCK rat livers. A 1.4-, 2.0-, and 2.3-fold increase in protein levels were detected in PCK rat livers for Mrp3, Ostβ, and Mdr1b, respectively, but these differences were not statistically significant (Figure 3). In addition, protein levels of Oatp1a1 and Oatp1b2 were decreased by 1.6- and 1.7-fold, respectively, in PCK rat livers, but differences were not significant (Figure 3). Proteomics data showed a decrease in Oatp1a1, Ntcp, and Mrp2 with a PCK/WT ratio (mean$\pm$S.D.) of 0.563$\pm$0.038, 0.691$\pm$0.097, and 0.368$\pm$0.098, respectively, but only Oatp1a1 and Mrp2 were significantly different (Figure 4). Bsep protein expression was unchanged in PCK compared to WT rat livers (Figure 4). Oatb1b2, Oatp1a4, and Mrp3 could not be detected with the selected sequence peptides (Table 1).

Total glutathione (GSH + GSSG) Concentrations in Bile and Livers from WT and PCK Rats. Biliary total glutathione concentrations were reduced in PCK compared to WT rats (Figure 5A). No significant changes in hepatic total glutathione concentrations were detected in PCK compared to WT rats (Figure 5B).

Outflow Perfusate and Biliary Excretion Rates of CDF in *ex situ* Isolated Perfused Livers (IPLs) from WT and PCK Rats. LDH release from IPLs into outflow perfusate was negligible (<2% cytotoxicity, data not shown). To investigate whether changes in transporter expression in PCK rat livers affected substrate transport at a functional level, the hepatobiliary disposition of CDF was measured in *ex situ* IPLs. Although the body weight of WT and PCK rats was similar (458±34 g and 495±3.6 g, respectively), PCK rat livers (28.1±9.1 g) were approximately 2-fold larger than WT rat livers (15.4±1.0 g). CDF outflow perfusate rate vs. time data were similar between WT and PCK rat IPLs, but the biliary excretion rates were markedly reduced in PCK IPLs (Figure 6). The first four data points for the biliary excretion rates in PCK rats were below the limit of quantitation and are, therefore, not shown in Figure 6.

Pharmacokinetic Modeling. The WT and PCK outflow perfusate and biliary excretion rate vs. time data were well described by a model consisting of a single hepatocellular compartment (Figures 1 and 6). A lag time for movement of CDF from the hepatocellular space into bile was incorporated only in the model describing the PCK rat IPL data. The CDF biliary excretion rate constant (K_{Bile}) was significantly decreased in PCK IPLs by more than an order of magnitude (Table 2). The CDF uptake clearance (CL_{UP}) was decreased approximately 2-fold in and the basolateral efflux rate constant (K_{BL}) of CDF was significantly increased in PCK IPLs.

8. Discussion

Previous studies suggest that the hepatobiliary disposition of endogenous and exogenous substrates may be altered in rodents with PKD. For example, various bile acids including unconjugated chenodeoxycholic acid (CDCA), deoxycholic acid (DCA), and lithocholic acid (LCA), and the glycine and taurine conjugates of CDCA (GCDCA and TCDCA, respectively) and DCA (GDCA and TDCA, respectively) are significantly increased in the serum and liver of PCK rats (Munoz-Garrido et al., 2015; Brock et al., 2018), a rodent model of ADPKD (Katsuyama et al., 2000; Masyuk et al., 2004. Although no significant increases in ALT, aspartate aminotransferase, or the bile acid synthesis Cyp7a1 mRNA levels were detected in PCK rats (Munoz-Garrido et al., 2015), serum bilirubin concentrations were increased in PCK rats, suggestive of impaired Mrp2 function (Mason et al., 2010; Shimomura et al., 2015). Previous published data have shown that liver disease can affect hepatic transporter expression and function (Thakkar et al., 2017). The present study is the first to report altered protein expression and function of hepatic transporters in PCK rat livers.

The significant decrease in protein levels of Oatps in PCK rat livers was notable; Oatp1a4 measured by immunoblot and Oatp1a1 measured by immunoblot and LC-MS/MS were both decreased (Figures 3 and 4). Decreased Oatp protein levels in PCK rat livers could have a significant impact on the hepatic disposition of Oatp substrates in this rodent model. The clinical implications of decreased hepatic OATP protein levels could lead to altered efficacy or toxicity of some drugs, particularly in patients with ADPKD. This warrants further investigation. Significant downregulation of Abcc2 and a 3-fold decrease in Mrp2 protein levels was observed in PCK compared to WT rat livers (Figures 2-4). In contrast, Abcc3 gene expression was significantly increased in PKC rat livers. However, due to variability in protein levels, Mrp3 protein was not significantly different (Figures 2 and 3).

Biliary excretion of endogenous total glutathione (GSH + GSSG) was markedly reduced in PCK rats (Figure 5A), consistent with decreased Mrp2 protein levels. Similar results were observed in Mrp2-deficient TR^- rats (Oude Elferink et al., 1989). Interestingly, hepatic total glutathione concentrations were not significantly different in PCK compared to WT rats. Liver weights were greater in PCK rats, which might be due, in part, to the hepatic cysts that amount to 3.92 mL, on average, in 16-week-old PCK rats (Brock et al., 2017), or up to 15% of the liver tissue (Munoz-Garrido et al., 2015).

Altered hepatobiliary disposition of CDF in PCK IPLs clearly demonstrated that changes in protein expression translated to functional changes. CDF is a fluorescent anion that is excreted unchanged into bile by Mrp2 in rats (Zamek-Gliszczynski et al., 2003). CDF is also a substrate for Oatp1a1-mediated hepatic uptake and undergoes basolateral efflux by Mrp3 when Mrp2 function is impaired (Xiong et al., 2000; Zamek-Gliszczynski et al., 2003; Chandra et al., 2005b; Nezasa et al., 2006). The concentration of CDF (~1 μM) employed in the IPL studies was well below the reported K_m (22 ±10 μM) for uptake in rat hepatocytes (Zamek-Gliszczynski et al., 2003). A pharmacokinetic model was employed to evaluate changes in the hepatic uptake, biliary excretion and basolateral efflux of CDF. In general, the model adequately described the data with low CV% (< 50%). Pharmacokinetic modeling revealed that the hepatic uptake clearance and biliary excretion rate constant of CDF were decreased by 1.9- and 28-fold, respectively, consistent with the observed decrease in Oatp1a1 and Mrp2 protein levels in PCK rat livers (Table 2, Figure 3 and 5). Interestingly, incorporation of a lag time for movement of CDF from the liver to bile was required only in the PCK rat livers in order to adequately describe the data. One possible explanation for the lag time may be the dilated cystic bile ducts in PCK rats (Masyuk et al., 2004). In addition, the basolateral efflux rate constant of CDF, presumably

mediated by Mrp3, was increased by 2-fold. Mrp3 serves as a compensatory route for excretion of Mrp2 substrates when biliary excretion is impaired (Konig et al., 2000; Ogawa et al., 2002; Chandra et al., 2004).

These results reveal that protein levels and function of hepatic drug transporters is altered in PCK rats. If similar alterations in hepatic transporters occur in humans with PKD, these patients may be predisposed to liver injury by drugs that inhibit hepatic transporters, such as tolvaptan (Slizgi et al., 2016). Patients with ADPKD treated with tolvaptan have an increased risk of drug-induced liver injury and may have altered drug disposition compared to the non-ADPKD population (Torres et al., 2012; Torres et al., 2017).

In conclusion, these novel findings indicate that significant alterations in hepatic transporter expression and function in PCK rat livers lead to decreased hepatic uptake and impaired biliary excretion of CDF, a probe substrate of organic anion transporters. Impaired Oatp-mediated hepatic uptake and Mrp2-mediated biliary excretion of drugs and metabolites have important implications for the use of this rodent model in drug development investigations. Furthermore, altered hepatic transporter function can influence the hepatobiliary disposition of endogenous (*e.g.,* bile acids) and exogenous compounds, and may be a predisposing risk factor in drug-induced liver injury.

9. Acknowledgments

The authors gratefully acknowledge Certara for providing academic research licenses for Phoenix® software as part of the Center of Excellence program for educational institutions. Liver tissues from WT and PCK rats (16 weeks) were obtained from experiments conducted by Dr. Jason R. Slizgi. We thank Dr. Noora Sjöstedt for her support with the visual abstract.

10. Authorship Contributions

Participated in research design: Bezençon, Beaudoin, Roth, Brock and Brouwer

Conducted experiments: Bezençon, Beaudoin, and Ito

Performed data analysis: Beaudoin, Bezençon, Ito, Fu, Roth, Brock, and Brouwer

Wrote or contributed to the writing of the manuscript: Bezençon, Beaudoin, and Brouwer.

Edited and revised manuscript: Bezençon, Beaudoin, Ito, Fu, Roth, Brock, and Brouwer.

11. References

Beaudoin JJ, Bezencon J, Cao Y, Mizuno K, Roth SE, Brock WJ, and Brouwer KLR (2018) Altered hepatobiliary disposition of tolvaptan and selected tolvaptan metabolites in a rodent model of polycystic kidney disease. *Drug Metab Dispos* **47**:155-163.

Brock WJ, Beaudoin JJ, Slizgi JR, Su M, Jia W, Roth SE, and Brouwer KLR (2018) Bile acids as potential biomarkers to assess liver impairment in polycystic kidney disease. *Int J Toxicol* **37:**144-154.

Brouwer KLR and Thurman RG (1996) Isolated perfused liver, in: *Models for assessing Drug absorption and metabolism* (Borchardt RT, Smith PL, and Wilson G eds), pp 161-192, Springer US, Boston, MA.

Chandra P and Brouwer KLR (2004) The complexities of hepatic drug transport: current knowledge and emerging concepts. *Pharm Res* **21**:719-735.

Chandra P, Johnson BM, Zhang P, Pollack GM, and Brouwer KLR (2005a) Modulation of hepatic canalicular or basolateral transport proteins alters hepatobiliary disposition of a model organic anion in the isolated perfused rat liver. *Drug Metab Dispos* **33:**1238-1243.

Chandra P, Zhang P, and Brouwer KLR (2005b) Short-term regulation of multidrug resistance-associated protein 3 in rat and human hepatocytes. *Am J Physiol Gastrointest Liver Physiology* **288:**G1252-1258.

Chauveau D, Fakhouri F, and Grunfeld JP (2000) Liver involvement in autosomal-dominant polycystic kidney disease: therapeutic dilemma. *J Am Soc Nephrol* **11:**1767-1775.

Chebib FT and Torres VE (2016) Autosomal dominant polycystic kidney disease: core curriculum 2016. *Am J Kidney Dis* **67:**792-810.

Cnossen WR and Drenth JP (2014) Polycystic liver disease: an overview of pathogenesis, clinical manifestations and management. *Orphanet J Rare Dis* **9:**69.

Dawson PA, Lan T, and Rao A (2009) Bile acid transporters. *J Lipid Res* **50:**2340-2357.

Everson GT, Scherzinger A, Berger-Leff N, Reichen J, Lezotte D, Manco-Johnson M, and Gabow P (1988) Polycystic liver disease: quantitation of parenchymal and cyst volumes from computed tomography images and clinical correlates of hepatic cysts. *Hepatology* **8:**1627-1634.

Halvorson CR, Bremmer MS, and Jacobs SC (2010) Polycystic kidney disease: inheritance, pathophysiology, prognosis, and treatment. *Int J Nephrol Renovasc Dis* **3:**69-83.

Harris PC and Torres VE (2009) Polycystic kidney disease. *Annu Rev Med* **60:**321-337.

Hartung EA and Guay-Woodford LM (2014) Autosomal recessive polycystic kidney disease: a hepatorenal fibrocystic disorder with pleiotropic effects. *Pediatrics* **134:**e833-845.

Hobbs M, Parker C, Birch H, and Kenworthy K (2012) Understanding the interplay of drug transporters involved in the disposition of rosuvastatin in the isolated perfused rat liver using a physiologically-based pharmacokinetic model. *Xenobiotica* **42:**327-338.

Hogan MC, Abebe K, Torres VE, Chapman AB, Bae KT, Tao C, Sun H, Perrone RD, Steinman TI, Braun W, Winklhofer FT, Miskulin DC, Rahbari-Oskoui F, Brosnahan G, Masoumi A, Karpov IO, Spillane S, Flessner M, Moore CG, and Schrier RW (2015) Liver involvement in early autosomal-dominant polycystic kidney disease. *Clin Gastroenterol Hepatol* **13:**155-164 e156.

Jackson JP, Freeman K, Brouwer KR (2016) Basolateral Efflux Transporters: a potentially important pathway for the prevention of cholestatic hepatotoxicity. *Appl In Vitro Toxicol*

2:207- 216.

Katsuyama M, Masuyama T, Komura I, Hibino T, and Takahashi H (2000) Characterization of a novel polycystic kidney rat model with accompanying polycystic liver. *Exp Anim* **49:**51-55.

Konig J, Rost D, Cui Y, and Keppler D (1999) Characterization of the human multidrug resistance protein isoform MRP3 localized to the basolateral hepatocyte membrane. *Hepatology* **29**:1156–1163.

Lager DJ, Qian Q, Bengal RJ, Ishibashi M, and Torres VE (2001) The pck rat: a new model that resembles human autosomal dominant polycystic kidney and liver disease. *Kidney international* **59:**126-136.

Li N, Nemirovskiy OV, Zhang Y, Yuan H, Mo J, Ji C, Zhang B, Brayman TG, Lepsy C, Heath TG, and Lai Y (2008) Absolute quantification of multidrug resistance-associated protein 2 (MRP2/ABCC2) using liquid chromatography tandem mass spectrometry. *Anal Biochem* **380:**211-222.

Li N, Zhang Y, Hua F, and Lai Y (2009) Absolute difference of hepatobiliary transporter multidrug resistance-associated protein (MRP2/Mrp2) in liver tissues and isolated hepatocytes from rat, dog, monkey, and human. *Drug Metab Dispos* **37:**66-73.

Malinen MM, Ito K, Kang HE, Honkakoski P, and Brouwer KLR (2019) Protein expression and function of organic anion transporters in short-term and long-term cultures of Huh7 human hepatoma cells. *Eur J Pharm Sci* **130:**186-195.

Mason SB, Liang Y, Sinders RM, Miller CA, Eggleston-Gulyas T, Crisler-Roberts R, Harris PC, and Gattone VH, 2nd (2010) Disease stage characterization of hepatorenal fibrocystic pathology in the PCK rat model of ARPKD. *Anat Rec (Hoboken)* **293:**1279-1288.

Masyuk TV, Huang BQ, Masyuk AI, Ritman EL, Torres VE, Wang X, Harris PC, and Larusso NF (2004) Biliary dysgenesis in the PCK rat, an orthologous model of autosomal recessive polycystic kidney disease. *Am J Pathol* **165:**1719-1730.

Miranda SR, Lee JK, Brouwer KL, Wen Z, Smith PC, and Hawke RL (2008) Hepatic metabolism and biliary excretion of silymarin flavonolignans in isolated perfused rat livers: role of multidrug resistance-associated protein 2 (Abcc2). *Drug Metab Dispos* **36:**2219-2226.

Munoz-Garrido P, Marin JJ, Perugorria MJ, Urribarri AD, Erice O, Saez E, Uriz M, Sarvide S, Portu A, Concepcion AR, Romero MR, Monte MJ, Santos-Laso A, Hijona E, Jimenez-Aguero R, Marzioni M, Beuers U, Masyuk TV, LaRusso NF, Prieto J, Bujanda L, Drenth JP, and Banales JM (2015) Ursodeoxycholic acid inhibits hepatic cystogenesis in experimental models of polycystic liver disease. *J Hepatol* **63:**952-961.

Nezasa K, Tian X, Zamek-Gliszczynski MJ, Patel NJ, Raub TJ, and Brouwer KLR (2006) Altered hepatobiliary disposition of 5 (and 6)-carboxy-2',7'-dichlorofluorescein in Abcg2 (Bcrp1) and Abcc2 (Mrp2) knockout mice. *Drug Metab Dispos* **34:**718-723.

Ogawa K, Suzuki H, Hirohashi T, Ishikawa T, Meier PJ, Hirose K, Akizawa T, Yoshioka M, and Sugiyama Y (2000) Characterization of inducible nature of MRP3 in rat liver. *Am J Physiol* **278**:G438–G446.

Oude Elferink RPJ, Ottenhoff R, Liefting W, de Haan J, Jansen PLM (1989) Hepatobiliary Transport of glutathione and glutathione conjugate in rats with hereditary hyperbilirubinemia. *J Clin Invest* **84**:476-483.

Pfeifer ND, Bridges AS, Ferslew BC, Hardwick RN, and Brouwer KLR (2013) Hepatic basolateral efflux contributes significantly to rosuvastatin disposition II: characterization

of hepatic elimination by basolateral, biliary, and metabolic clearance pathways in rat isolated perfused liver. *J Pharmacol Exp Ther* **347:**737-745.

Prasad B, Evers R, Gupta A, Hop CE, Salphati L, Shukla S, Ambudkar SV, and Unadkat JD (2014) Interindividual variability in hepatic organic anion-transporting polypeptides and P-glycoprotein (ABCB1) protein expression: quantification by liquid chromatography tandem mass spectroscopy and influence of genotype, age, and sex. *Drug Metab Dispos* **42:**78-88.

Pretlow II TG and Pretlow TP (1987) Cell separation: methods and selected applications, pp 1-20, Harcourt Brace Jovanovich.

Qian Q, Li A, King BF, Kamath PS, Lager DJ, Huston J, 3rd, Shub C, Davila S, Somlo S, and Torres VE (2003) Clinical profile of autosomal dominant polycystic liver disease. *Hepatology* **37:**164-171.

Ruh H, Salonikios T, Fuchser J, Schwartz M, Sticht C, Hochheim C, Wirnitzer B, Gretz N, and Hopf C (2013) MALDI imaging MS reveals candidate lipid markers of polycystic kidney disease. *J Lipid Res* **54:**2785-2794.

Salam M and Keeffe EB (1989) Liver cysts associated with polycystic kidney disease: role of Tc-99m hepatobiliary imaging. *Clin Nucl Med* **14:**803-807.

Schenker NaG, J.F. (2001) On judging the significance of differences by examining overlap between confidence intervals. *The American Statistician* **55:**182-186.

Shimomura Y, Brock WJ, Ito Y, and Morishita K (2015) Age-related alterations in blood biochemical characterization of hepatorenal function in the PCK rat: A model of polycystic kidney disease. *Int J Toxicol* **34:**479-490.

Shoaf SE, Ohzone Y, Ninomiya S, Furukawa M, Bricmont P, Kashiyama E, and Mallikaarjun S (2011) In vitro P-glycoprotein interactions and steady-state pharmacokinetic interactions between tolvaptan and digoxin in healthy subjects. *J Clin Pharmacol* **51:**761-769.

Slizgi JR, Lu Y, Brouwer KR, St Claire RL, Freeman KM, Pan M, Brock WJ, and Brouwer KLR (2016) Inhibition of human hepatic bile acid transporters by tolvaptan and metabolites: contributing factors to drug-induced liver injury? *Toxicol Sci* **149:**237-250.

Thakkar N, Slizgi JR, and Brouwer KLR (2017) Effect of liver disease on hepatic transporter expression and function. *J Pharm Sc* **106:**2282-2294.

Torres VE, Chapman AB, Devuyst O, Gansevoort RT, Grantham JJ, Higashihara E, Perrone RD, Krasa HB, Ouyang J, Czerwiec FS, and Investigators TT (2012) Tolvaptan in patients with autosomal dominant polycystic kidney disease. *N Engl J Med* **367:**2407-2418.

Torres VE, Chapman AB, Devuyst O, Gansevoort RT, Perrone RD, Koch G, Ouyang J, McQuade RD, Blais JD, Czerwiec FS, Sergeyeva O, and Investigators RT (2017) Tolvaptan in later-stage autosomal dominant polycystic kidney disease. *N Engl J Med* **377:**1930-1942.

Uchida Y, Ohtsuki S, Katsukura Y, Ikeda C, Suzuki T, Kamiie J, and Terasaki T (2011) Quantitative targeted absolute proteomics of human blood-brain barrier transporters and receptors. *J Neurochem* **117:**333-345.

US Food & Drug Administration (FDA). Drug Approval Package: Jynarque (tolvaptan). Created June 8, 2018. https://www.accessdata.fda.gov/drugsatfda_docs/nda/2018/204441Orig1s000TOC.cfm. Accessed February 14, 2019.

Wang L, Prasad B, Salphati L, Chu X, Gupta A, Hop CE, Evers R, and Unadkat JD (2015) Interspecies variability in expression of hepatobiliary transporters across human, dog, monkey, and rat as determined by quantitative proteomics. *Drug Metab Dispos* **43:**367-374.

Watanabe T, Kusuhara H, Maeda K, Shitara Y, and Sugiyama Y (2009) Physiologically based pharmacokinetic modeling to predict transporter-mediated clearance and distribution of pravastatin in humans. *J Pharmacol Exp Ther* **328:**652-662.

Watkins PB, Lewis JH, Kaplowitz N, Alpers DH, Blais JD, Smotzer DM, Krasa H, Ouyang J, Torres VE, Czerwiec FS, and Zimmer CA (2015) Clinical pattern of tolvaptan-associated liver injury in subjects with autosomal dominant polycystic kidney disease: analysis of clinical trials database. *Drug safety* **38:**1103-1113.

Xiong H, Turner KC, Ward ES, Jansen PL, and Brouwer KL (2000) Altered hepatobiliary disposition of acetaminophen glucuronide in isolated perfused livers from multidrug resistance-associated protein 2-deficient TR(-) rats. *J Pharmacol Exp Ther* **295:**512-518.

Zamek-Gliszczynski MJ, Xiong H, Patel NJ, Turncliff RZ, Pollack GM, and Brouwer KL (2003) Pharmacokinetics of 5 (and 6)-carboxy-2',7'-dichlorofluorescein and its diacetate promoiety in the liver. *J Pharmacol Exp Ther* **304:**801-809.

Zhang A, Jia Y, Xu Q, Wang C, Liu Q, Meng Q, Peng J, Sun H, Sun P, Huo X, and Liu K (2016) Dioscin protects against ANIT-induced cholestasis via regulating Oatps, Mrp2 and Bsep expression in rats. *Toxicol Appl Pharmacol* **305:**127-135.

12. Footnotes

This work was supported, in part, by Otsuka Pharmaceutical Development & Commercialization, Inc., and the National Institutes of Health National Institute of General Medical Sciences [Grants R01 GM041935 and R35 GM122576].

This work was presented, in part, at the 10th Biomedical Transporter Conference, the American Association of Pharmaceutical Scientists Transporter Workshop 2018, and the 2018 Drug Metabolism Gordon Research Conference.

Any opinions, findings, conclusions, or recommendations expressed in this publication are those of the authors and do not necessarily reflect the views of the Otsuka Pharmaceutical Group or the National Institutes of Health.

DMD Fast Forward. Published on June 3, 2019 as DOI: 10.1124/dmd.119.086785
This article has not been copyedited and formatted. The final version may differ from this version.

13. Figure Legends

Figure 1. Model Scheme Depicting the Disposition of CDF in Rat Isolated Perfused Livers. The rate of change in the mass of CDF in the perfusate entering the sinusoidal compartment in relation to time, dX_{in}/dt, was described by the product of the perfusate flow rate (Q) and the inflow perfusate concentration (C_{in}). The product of Q and the outflow perfusate concentration (C_{out}) was used to describe the rate of change in the mass of CDF in the perfusate leaving the sinusoidal compartment in relation to time, dX_{out}/dt. The concentration in the sinusoidal compartment, C_S, was assumed to be equal to C_{out}. While CL_{UP} described the clearance of CDF from the sinusoidal to the hepatocellular space, K_{BL} and K_{Bile} denoted the rate constants for the basolateral and biliary efflux from the hepatocellular space, respectively. The product of K_{Bile} and the hepatocellular amount of CDF (X_H) was used to describe the biliary excretion rate, dX_{Bile}/dt.The incorporation of transit compartments ($X_{Bile,1-5}$) and a transit rate constant ($K_{Lag,Bile}$) subsequent to the biliary excretion of CDF (highlighted by the gray shading) improved the model fit to the biliary excretion rate data for polycystic kidney rats. X_S and V_S represent the mass of CDF in, and the volume of, the sinusoidal space, respectively.

Figure 2. **Transporter Gene Expression in WT Compared to PCK Rat Livers.** Quantitation of mRNA isolated from liver tissue of wild-type (WT) and polycystic kidney (PCK) rats. Data were normalized to Gapdh and are shown as the fold change from WT ($2^{-\Delta\Delta Ct}$, fold difference in WT relative to PCK) mean ± SD (*n* = 3 per group). Statistically significant differences were determined by an unpaired, two-tailed *t*-test (*$p < 0.05$, WT vs. PCK).

Figure 3. **Transporter Protein Expression in WT Compared to PCK Rat Livers.** A) Immunoblots of liver tissue samples from wild-type (WT) and polycystic kidney (PCK) rats (*n* = 3 per group). Each protein was analyzed on a separate membrane and Na^+/K^+ ATPase was

probed on the same blot as the respective protein. B) Results of integrated optical density analysis of western blots prepared from WT and PCK rat liver tissue samples (n = 3 per group). Data were normalized to Na^+/K^+ ATPase and are shown as mean ± SD. Statistically significant differences were determined by an unpaired, two-tailed t-test (*$p < 0.05$, WT vs. PCK).

Figure 4. LC-MS/MS-Based Proteomic Analysis of Transporter Protein Expression in WT Compared to PCK Rat Livers. Bars represent the mean ± SD of the polycystic kidney (PCK)/wild-type (WT) ratio based on the average signal from three product ions (see **Table 1**) (n = 3 rats per group). Statistically significant differences compared to the Na^+/K^+ ATPase PCK/WT ratio were determined by an unpaired, two-tailed t-test corrected for multiple comparisons by using the Bonferroni-Dunn method (*$p < 0.05$). Transport proteins that were not detected by LC-MS/MS in the WT and PCK rat liver tissue samples are not shown in this figure.

Figure 5. Total Glutathione (GSH + GSSG) Concentrations in Bile and Liver of WT and PCK Rats. A) Biliary total glutathione concentrations (mmol/L) and B) hepatic total glutathione concentrations (μmol/g) in WT (black bars) and PCK rats (white bars) (n = 3 per group). Data are shown as mean ± SD. Statistically significant differences were determined by an unpaired, two-tailed t-test (*$p < 0.05$, WT vs. PCK).

Figure 6. **Outflow perfusate and biliary excretion rates of CDF in ex situ isolated perfused livers (IPLs) from WT and PCK rats.** Observed outflow perfusate rate of 5(6)-carboxy-2',7'-dichlorofluorescein (CDF) (open circles) and CDF biliary excretion rate (closed circles) in (A) wild-type (WT) and (B) polycystic kidney (PCK) IPLs (mean ± SD; n = 3 per group). Livers were perfused with 1 μM CDF-containing perfusate for 30 min followed by

perfusion with CDF-free perfusate for an additional 20 min, represented by the black and gray bars, respectively. The fit of the pharmacokinetic model, based on the scheme depicted in Figure 1, to the biliary excretion (solid curves) and outflow perfusate (dashed curves) rate vs. time profiles are plotted with the mean data. The first four data points for the biliary excretion of CDF in PCK IPLs were below the limit of quantitation and are not shown.

DMD Fast Forward. Published on June 3, 2019 as DOI: 10.1124/dmd.119.086785
This article has not been copyedited and formatted. The final version may differ from this version.

14. Tables

Table 1. Selected reaction monitoring (SRM) parameters of peptides used for targeted analysis of hepatobiliary transporters (Oatp1a1, Oatp1a4, Oatp1b2, Ntcp, Mrp3, Mrp2, Bsep, Na^+/K^+ ATPase) for LC-MS/MS-based proteomic analysis in wild-type (WT) and polycystic kidney (PCK) rat livers. The labeled amino acid residue of the internal standard is shown in bold with an asterisk *.

Protein	Probe Sequence	SRM Transition			
		Parent Ion (Q1)	Product Ions (Q3)		
			1	2	3
***Slc21a1* / Oatp1a1**	EENLGITK	452.2	645.4	531.4	418.3
	EENLGIT**K***	456.2	653.4	539.4	426.3
***Slco1a4* / Oatp1a4**	TFQFPGDIESSK	678.4	832.4	735.4	563.4
	TFQFPGDIESS**K***	682.4	840.4	743.4	571.4
***Slco1b2* / Oatp1b2**	SVQPELK	400.8	614.4	486.3	260.2
	SVQPEL**K***	404.8	622.4	494.3	268.2
***Slc10a1*/ Ntcp**	AAATEDATPAALEK	679.9	729.4	915.5	628.4
	AAATEDATPAALE**K***	683.9	737.4	923.5	636.4
***Abcc3* / Mrp3**	FYVATSR	422.4	696.4	533.3	434.2
	FYVATS**R***	427.4	706.4	543.3	444.2
***Abcc2* / Mrp2**	LTIIPQDPILFSGSLR	885.5	989.6	1329.7	666.4
	LTIIPQDPILFSGSL**R***	890.5	999.6	1339.7	676.4
***Abcb11* / Bsep**	STSIQLLER	523.8	530.3	658.4	858.5
	STSIQLLE**R***	528.8	540.3	668.4	868.5
***Na^+/K^+ ATPase* / Na^+/K^+ ATPase**	AAVPDAVGK	414.2	685.4	586.3	374.2
	AAVPDAVG**K***	418.2	693.4	594.3	382.2

DMD Fast Forward. Published on June 3, 2019 as DOI: 10.1124/dmd.119.086785
This article has not been copyedited and formatted. The final version may differ from this version.

Table 2. Pharmacokinetic parameter estimates describing CDF disposition in single-pass isolated perfused livers from WT and PCK rats. Data represent mean ± SD (*n* = 3). NA = not applicable. Statistically significant differences were based on nonoverlapping 95% confidence intervals: **p*<0.05, WT vs PCK.

Pharmacokinetic Parameter Estimates								
	Wild-type (WT)				Polycystic Kidney (PCK)			
Parameter	**Estimate**	**CV%**	**2.5% CI**	**97.5% CI**	**Estimate**	**CV%**	**2.5% CI**	**97.5% CI**
CL_{UP} (mL/min)	8.80	10.9	6.74	10.9	4.69*	15.5	3.05	6.34
K_{BL} (min^{-1})	0.0828	13.5	0.0588	0.107	0.162*	10.3	0.125	0.200
K_{Bile} (min^{-1})	0.0506	12.5	0.0371	0.0641	0.00181*	45.5	0	0.00367
$K_{Lag,Bile}$ (min^{-1})	NA				0.136	23.8	0.0630	0.209

DMD Fast Forward. Published on June 3, 2019 as DOI: 10.1124/dmd.119.086785
This article has not been copyedited and formatted. The final version may differ from this version.

15. Figures (available in pdf format upon request)

Figure 1:

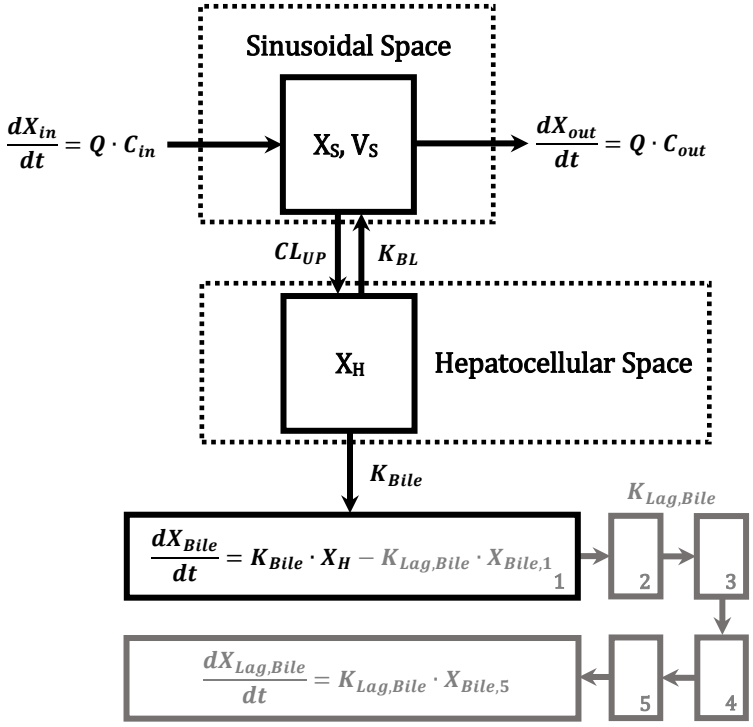

DMD Fast Forward. Published on June 3, 2019 as DOI: 10.1124/dmd.119.086785
This article has not been copyedited and formatted. The final version may differ from this version.

Figure 2:

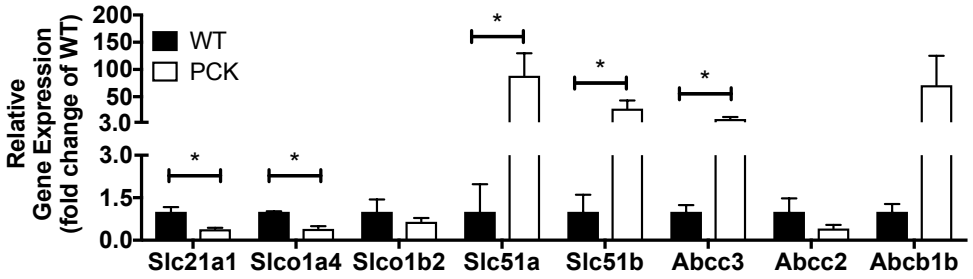

DMD Fast Forward. Published on June 3, 2019 as DOI: 10.1124/dmd.119.086785
This article has not been copyedited and formatted. The final version may differ from this version.

Figure 3:

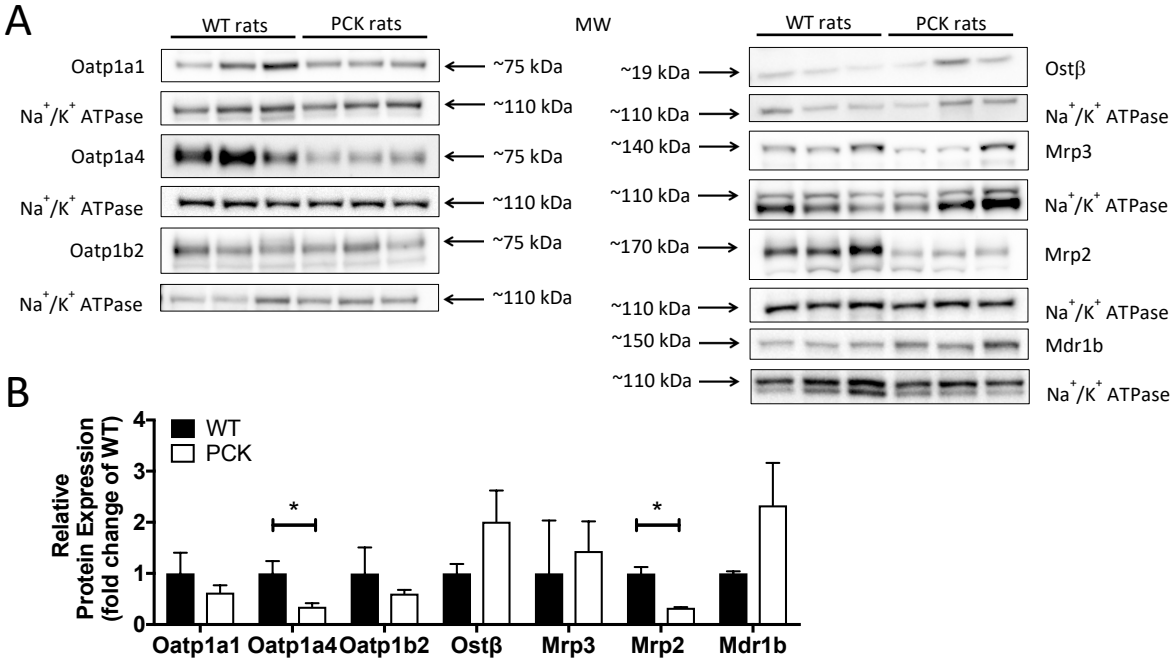

DMD Fast Forward. Published on June 3, 2019 as DOI: 10.1124/dmd.119.086785
This article has not been copyedited and formatted. The final version may differ from this version.

Figure 4:

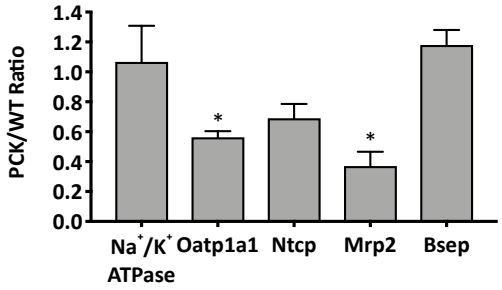

DMD Fast Forward. Published on June 3, 2019 as DOI: 10.1124/dmd.119.086785
This article has not been copyedited and formatted. The final version may differ from this version.

Figure 5:

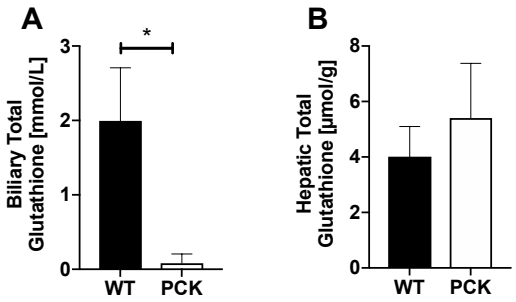

DMD Fast Forward. Published on June 3, 2019 as DOI: 10.1124/dmd.119.086785
This article has not been copyedited and formatted. The final version may differ from this version.

Figure 6: